The 2009 IEEE/RSJ International Conference on
Intelligent Robots and Systems
October 11-15, 2009 St. Louis, USA

Kinematic analysis for a novel design of MRI-compatible torque sensor

Pierre Renaud and Michel de Mathelin

Abstract— **In this paper, the design of a novel MRI-compatible torque sensor is proposed. The sensor is based on an optical measurement, with a particular architecture to provide a very low cross-sensitivity. Its structure allows to simultaneously tune the sensor stiffness and the measurement amplitude of the optical sensor. To do so, kinematic singularities of parallel structures are used as well as the principles of dissociated metrology structure. The design of the sensor is first introduced by a kinematic analysis, before detailing its behavior using Finite Element Analysis. A prototype is finally introduced with first experimental results.**

I. INTRODUCTION

MRI-guided robotic procedures are of great interest from a medical point of view because of the level of details that can be obtained, and several robotized surgical gestures are now considered under MRI guidance, like brachytherapy [1] or percutaneous procedures [2].

Designing perception systems for MRI compatible robots is not an easy task because of the strong magnetic field. Optical sensors have appeared to be a promising choice: the principle is to obtain a measurement using optical fibers, without any active component in the magnetic field. Even though other technologies could be considered in some cases [3], [4] many authors have considered the development of optical sensors, *i.e.* using optical fibers. One may notice that the interest of optical sensors also exists for fMRI application such as brain mapping [5], [6] and in other contexts because of harsh environments and operations [7].

Optical sensors can be divided in two families. In the first one, sensors use the properties of the optical fiber itself to get a measurement [8], [9], [10], notably by using fiber Bragg gratings. In the second family, sensors use optical fibers only to transport light. The measurement is performed by using an additional sensing element, and comparing the emitted and returned light intensity. The sensing element may be a grating, to use Moire fringe [11], a mask [12], [13] or a mirror [14].

In the following, we focus on the second family, because of their simplicity and their moderate cost. More precisely, we focus on the force/torque sensors proposed on that principle.

Optical force/torque sensors are based on a compliant mechanical structure that must convert the force/torque applied on the sensor end-effector in a displacement detected by a variation of light intensity. The design of a sensor therefore consists in the selection of an adequate mechanical structure, the sensing element and its location with respect to the mechanical structure. When the sensor must be sensitive to a specific component of the wrench applied on its end-effector, for instance a single component of torque, several requirements have to be fulfilled by the sensor structure:

- no sensitivity must be exhibited to force/torque components other than the one to measure, *i.e* no cross-sensitivity
- stiffness must be large enough for the degree of freedom to measure, so that it does not introduce a compliance in the mechanism that could modify its control
- displacements of the sensor structure must be large enough to be estimated with the sensing element
- eigenfrequencies must be compatible with the application, to avoid any sensor resonance during the control of the mechanism on which it is mounted.

These constraints must be simultaneously satisfied, and it can be difficult to ensure in the same time the value of the stiffness and the amplitude of the sensor deformation for the measurement, as outlined in [15].

In the pioneer works on force sensors compatible with MRI [12], [16], six degrees of freedom (dof) force sensors are considered. The design of the compliant mechanical structure is then introduced qualitatively. Tada *et al* [17] consider the assembly of simple parallel plate structures to create the sensor structure. In [18], thin blades are considered and assembled for a 2-dof sensor. In both cases, only a qualitative analysis is performed, and as outlined by [19], in the second case the cross-sensitivity is actually high. The analysis of the sensor compliant mechanical structure is then performed using a Pseudo Rigid Body Model (PRBM [20]). With the same approach, a simple planar design for a torque sensor is introduced, with additional Finite Element Analysis (FEA).

In this paper, the PRBM approach is also chosen to perform the kinematic analysis of the sensor. Indeed, we propose a novel design by combining in a PRBM framework the principle of dissociated metrology structure [21] with the use of kinematic singularities. The sensor is composed of two compliant structures in parallel, with mechanisms close to serial and parallel kinematic singularities so that the sensor sensitivity and the cross-sensitivity can be optimized simultaneously. We focus on the design of a torque sensor compatible with MRI, for haptic applications for instance in fMRI.

In the second section, the kinematic properties used to propose the torque sensor are first presented. Then in the third section its main properties are described using FEA. In

P. Renaud and M. de Mathelin are with LSIIT, Strasbourg University - CNRS, 67412 Illkirch, France {pierre.renaud , dematheli n}@lsiit.u-strasbg.fr

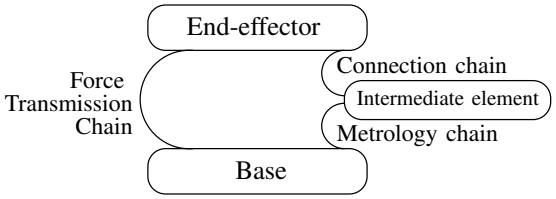

Fig. 1. Kinematic decomposition in the case of a dissociated metrology structure.

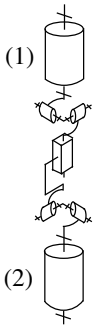

Fig. 2. Kinematic scheme of a possible torque sensor.

the fourth section first results obtained with a prototype are given, before concluding.

II. Dissociated metrology and kinematic singularities

A. Dissociated metrology structure

As mentioned in the first section, we consider the design of a torque sensor for haptic applications. To minimize the cross-sensitivity of the torque sensor, we propose to use the concept of dissociated metrology structure introduced in [21] for the design of high accuracy measurement machines. To do so, the sensor is composed of three kinematic chains (Fig. 1).

The end-effector is the element on which the external forces are exerted, and in particular the torque to be measured. This element is connected to the base by a kinematic chain designated as the *force transmission chain*. The *metrology chain* is dedicated to the evaluation of the torque applied on the end-effector. This kinematic chain is however not connected directly to the end-effector but through a *connection chain*.

The concept of dissociated metrology structure is based on two properties. First, the metrology chain must not use any hypothesis about the geometry of the force transmission chain to perform the evaluation of the end-effector displacement. In other words, the estimation of the end-effector displacement must be valid even in presence of displacements due to force/torque components other than the torque to be measured. Second, the end-effector of the metrology chain must not be submitted to deformations that could cause loss of measurement accuracy. This is the role of the connection chain.

Initially, the dissociated metrology structure principle does not concern compliant structures. Therefore, it is also considered that the force transmission chain is the kinematic chain by which the wrench on the end-effector is transmitted to the base of the sensor. The metrology chain is not designed to transmit any forces. In our context, both kinematic chains are compliant mechanisms. The force transmission chain will have the higher stiffness, so that forces exerted on the sensor end-effector are mostly supported by this kinematic chain.

For sake of clarity, an example of torque sensor based on the previous principles is given in Fig. 2. The force transmission chain (1) is reduced to a revolute joint, as well as the metrology chain (2). The connection chain is composed of two universal joints connected by a prismatic joint. With such a structure, the rotation of the end-effector is transmitted to the metrology chain. A translation of the axis of revolute joint (1) will not induce any modification of the position of revolute joint (2). Therefore, if for instance the torque applied on the sensor end-effector is combined with forces perpendicular to the revolute joint axis, displacement of the revolute joint (1) will occur, but without modification of the rotation measured on the revolute joint (2).

In the third section, the nature of the force transmission, metrology and connection chains will be discussed in details. We now introduce the kinematics properties that will be used for the selection of force transmission and metrology chains.

B. Parallel singularities

For stiffness reasons, we consider the force transmission chain as a closed-loop mechanism. From a kinematic point of view, the force transmission chain must therefore be in our context a parallel structure with the behavior of a revolute joint. The existence of small displacements for a closed-loop mechanism, when its actuators are blocked, has been widely studied in the field of parallel mechanisms. Such a situation is usually avoided, since that means that a mechanism would have uncontrollable movements. With $\dot{\mathbf{q}}$ the actuated joint velocities and $\dot{\mathbf{X}}$ the end-effector velocity, it is well-known that $\dot{\mathbf{X}} \neq \mathbf{0}$ can be obtained with $\dot{\mathbf{q}} = \mathbf{0}$ in a parallel singularity [22].

Working in the vicinity of parallel singularities has therefore been considered to amplify the measurement of forces exerted on a parallel structure [23], or to amplify actuators displacements [24], [25]. In our case, we remark that we can use results on the existence of parallel singularities to select closed-loop architectures that have locally the behavior of a compliant revolute joint.

A planar mechanism 3$\underline{\text{P}}$RR (Fig. 3) presents a parallel singularity when the distal linkages A_iB_i , $i \in [1, 3]$ intersect in one point E. In such a situation, and independently from the actuator directions $\mathbf{u_i}$, $i \in [1, 3]$, a torque applied on the center E of the end-effector cannot be counter-balanced by the distal linkages. A rotation of the end-effector can therefore appear.

Adding other legs to the mechanism does not modify this analysis, if the distal linkages still intersect in point E. With one more leg, one can for instance get the architecture

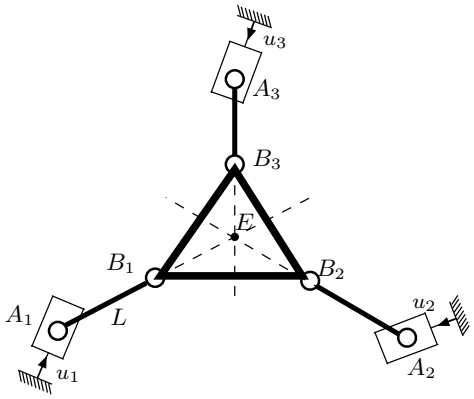

Fig. 3. Planar 3PRR in parallel singularity.

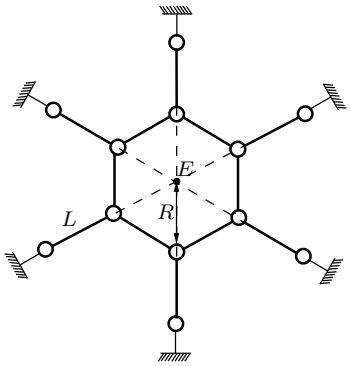

Fig. 4. Kinematic scheme of the force transmission chain.

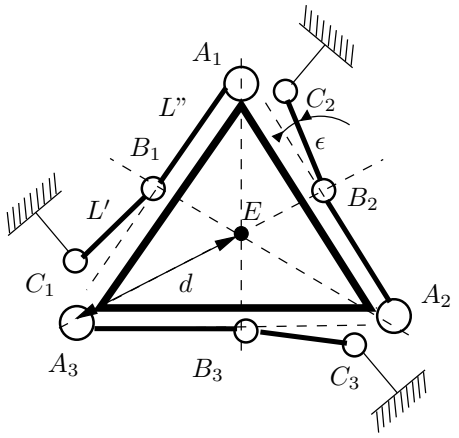

Fig. 5. Planar 3RRR close to serial singularity.

introduced in [19]. In this section, we have considered the PRBM of the compliant force transmission chain. Due to the material elasticity, the end-effector of this mechanism will present rotations and displacements due to the forces and moments other than the one to be measured. To limit these additional displacements, we consider a higher number of legs, and consider for symmetry considerations a force transmission chain composed of 6 legs (Fig. 4).

C. Serial singularities

The force transmission chain mainly allows a rotation along the torque sensor axis. This rotation is transmitted through the connection chain. Its amplitude, for a given torque range, depends on the stiffness needed for the sensor, given by the force transmission chain. Obtaining a sufficient measurement amplitude may therefore be difficult [15]. In [19], the light intensity variation is interestingly obtained using a mirror which displacement is maximized by mounting it at the maximum possible distance with respect to the rotation axis of the force transmission chain. In such a case, a linear increase of the displacement amplitude is obtained, which can remain limited, or causes a large increase of the sensor size.

We propose to use another kinematic property of parallel mechanisms, namely serial singularity, to amplify the rotation of the intermediate element, driven by the sensor end-effector displacement. To our knowledge, such an explicit use of serial singularity is novel. Ronchi *et al* [26] have considered working in the vicinity of a serial singularity, but in an inverse way, to maximize the resolution of a high accuracy mechanism.

Let us consider a simple parallel structure such as a 3RRR mechanism (Fig. 5), with the distal links $A_iB_i\,, i \in [1,3]$ parallel to the sides of the end-effector and the proximal links $B_iC_i\,, i \in [1,3]$ almost aligned with the distal links. The angle between the proximal and distal elements is denoted ϵ, the triangle $A_1A_2A_3$ is equilateral. The mechanism is in a serial singularity when the angle ϵ is equal to zero: no end-effector movement can then be obtained by the rotation of joints in C_i.

For the configuration represented in Fig. 5, the ratio between the rotational speed $\dot{\theta}$ of the end-effector and v_{B_i} the amplitude of the velocity of point $B_i\,, i \in [1,3]$ can easily be expressed in the case of a pure rotation of the end-effector:

$$v_{B_i} = \frac{d\dot{\theta}}{2\sin\epsilon} \tag{1}$$

Eq. (1) expresses also the relationship between a small rotation $\delta\theta$ and the displacement δu_{B_i} of the point B_i. The amplitude of the displacement at point B_i can therefore be tuned by choosing the value of the angle ϵ between two leg elements. If we choose to measure such a displacement with optical fibers and a mirror, like in [19], we can position the mirror at the end of the proximal links and finally maximize the measurement amplitude by working in the vicinity of a serial singularity.

Having introduced the kinematic properties that we will use to create a torque sensor, we now focus on the design of the compliant structures corresponding to the force transmission and metrology chains, and the choice of the connection chain.

III. Sensor design

In section 2, the design principles of the sensor have been presented using a rigid body approach. In this section, the

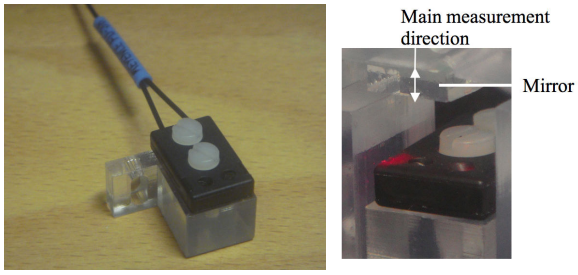

Fig. 6. Keyence FU-38 sensor head (left: the sensor head, right: configuration with a mirror)

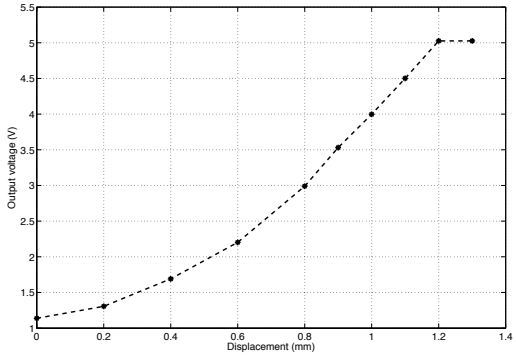

Fig. 7. Output voltage of the sensor.

analysis is achieved using Finite Element Analysis (FEA) to get an accurate evaluation of the sensor behavior.

A. Choice of sensor material and sensing element

For MRI compatibility, POM material is considered (Young modulus: 2800 MPa, Poisson ratio: 0.35, maximum stress: 68 MPa). The shape of the elements composing the sensor are chosen to allow a manufacturing with conventional CNC machining.

The sensing element is a Keyence FU-38 head (Fig. 6) associated to a Keyence FS-V31M amplifier. The FU-38 component is composed of two optical fibers, one for light emission and the other for the reception of the light returned to the sensor head by a reflective surface. Here a planar mirror will be used. The output of the FS-V31M is a voltage which is proportional to the received light intensity. Because of the sensor head geometry, the light variation detected by the sensor is mainly due to displacements of the mirror along its normal (Fig. 6). A rotation of the mirror can however also cause a variation of the light intensity. Displacements in directions parallel to the mirror plane, and rotation along its perpendicular do not influence the measurement. The measurement range is in the order of 1 mm (Fig. 7). The displacement-voltage relationship is however not linear on such a range, and we choose the range on which the sensitivity is the highest, *i.e.* 500 microns.

We consider the torque sensor to be grasped by a human hand. The torque range is chosen as a consequence equal to $\pm 5Nm$.

TABLE I

MAIN GEOMETRIC PARAMETERS FOR THE FORCE TRANSMISSION AND METROLOGY CHAINS

Parameter	Value
L	7 mm
L'	15 mm
L"	17 mm
ϵ	3°
R	15 mm
R'	27 mm
Minimum thickness of the flexure joints	
Force transmission chain	2 mm
Metrology chain	0.4 mm

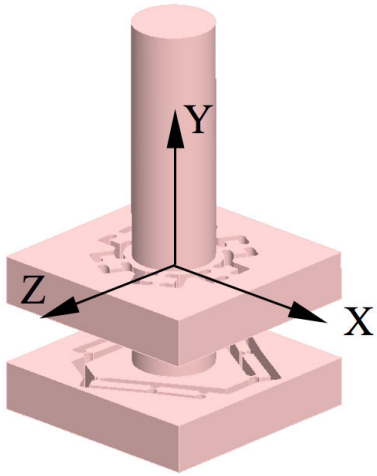

Fig. 8. CAD view of the compliant force transmission and metrology chains. Rigid connection between the two subsystems.

B. Force transmission and metrology chains

For the force transmission chain, the geometry of the compliant element (Fig. 8) is obtained by using the kinematic scheme in Fig. 4 with circular flexure joints for the revolute joints. In the same way, the compliant element corresponding to the metrology chain (Fig. 9) is based on the kinematic scheme in Fig. 5. The value of the main geometric parameters is reported in Table I.

In a first step, the end-effectors of the two subsystems are connected by a cylindrical element. The connection chain is thus considered to be a rigid connection (Fig. 8).

The force transmission and metrology chains are 15 mm thick. The application of a moment M_y along the Y direction (Fig. 8) equal to 5 Nm then creates a rotation equal to 4.10^{-3} rad and a displacement at the outer radius of the force transmission end-effector equal to $60\,\mu m$. The displacement at the end of the proximal links, measured with the sensor head as proposed in section II.C., is equal in the same time to $285\,\mu m$. We here observe the amplification provided by the structure in the vicinity of a serial singularity.

A force applied in the X or Z direction induces displacements of the force transmission end-effector. This cross-sensitivity is not immaterial: a force equal to $10\,N$ is sufficient to modify by 1% the displacement that would

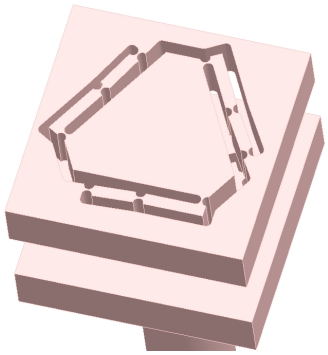

Fig. 9. CAD view of the compliant metrology chain.

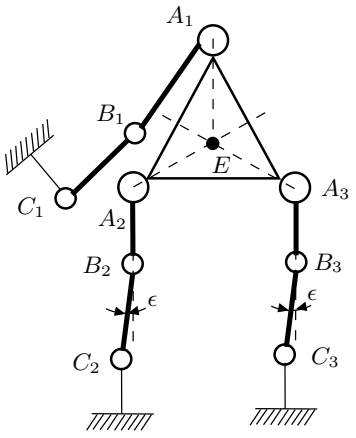

Fig. 10. Configuration for single sensor measurement.

be measured on the force transmission chain. Since the metrology chain has three degrees of freedom, we also observe displacements of its end-effector in this situation. Two alternate ways can be considered to take into account these displacements. The first one consists in the use of three sensors to measure the displacements of the three legs of the mechanism. The second one consists in the use of another configuration, as represented in Fig. 10. In this configuration, the sensor would measure the relative displacement of points B_2 and B_3, that can be demonstrated to be only dependent on the end-effector rotation. This way would allow a simpler and cheaper sensor. In this paper, we consider the use of multiple sensor elements, to be able experimentally to provide a more detailed analysis of the sensor behavior.

Moments applied on the sensor along the X or Z axes, *i.e.* in the plane of the sensor, cause rotations of the end-effector of the force transmission chain (Fig. 11). These rotations would induce additional perturbations on the measurement of the torque in the Y direction if the measurement was performed on that kinematic chain. With a rigid connection between the force transmission and metrology chains, the rotation is of the same amplitude (Fig. 11) on the metrology chain end-effector. We therefore have to include degrees of freedom in the connection chain to avoid the transmission of these additional rotations on the metrology chain. The nature

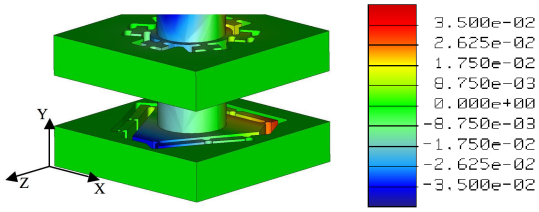

Fig. 11. Rigid connection chain. Displacements (in mm) in the Y direction for a moment $M_x = 5\,Nm$.

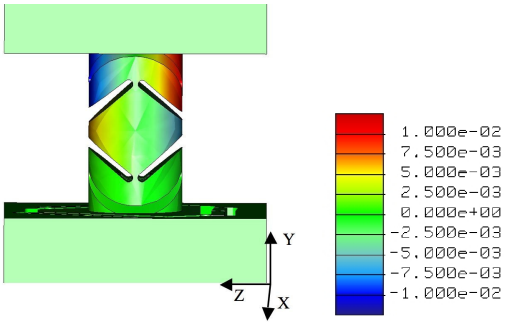

Fig. 12. Connection chain with two universal joints. Displacements (in mm) in the Y direction for a moment $M_x = 5\,Nm$.

of the connection chain is discussed in the next paragraph.

C. Selection of the transmission chain

1) Two universal joints: Using two universal joints as described in section II should allow to transmit the rotation along the Y direction, and avoid the transmission of moments in the X and Z directions. This kinematic behavior is confirmed by numerical simulations: in Fig. 12 one can notice that the gradient of displacement in the Y direction with respect to the Z coordinate becomes null on the metrology chain.

The use of two universal joints however introduces an additional flexibility to the structure that sharply reduces the rotation of the metrology chain rotation: the rotation amplitude is divided by 6 with respect to a rigid connection. We hence consider a simplified connection chain composed of a single universal joint.

2) Single universal joint: With a single universal joint in the connection chain, the application of a moment M_y equal to 5Nm induces a displacement to be measured equal to $200\,\mu m$. The visibility of the torque to measure is therefore still satisfactory. In the same time, moments along the X and Z axes induce rotations of the end-effector of the force transmission chain that are filtered by the universal joint: the rotation amplitude is divided by 6, and we almost only observe a translation of the metrology chain end-effector. As mentioned in section III.B., forces in the X and Z directions also cause translations of this element. As a conclusion, the use of a single universal joint allows us to distinguish the torque to measure from forces and moments in other directions. We therefore obtain a very low cross-sensitivity of the sensor, and the metrology chain can be tuned to get

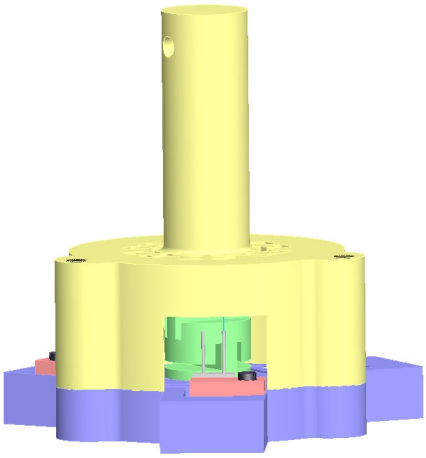

Fig. 13. CAD view of the sensor prototype.

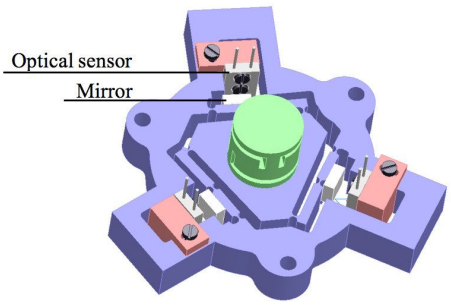

Fig. 14. Zoom on the metrology chain with the optical sensors (force transmission chain suppressed for visibility).

a measurement amplitude that allows the estimation of the torque applied on the sensor.

IV. Prototype design

A. CAD design

For a first evaluation, a prototype has been designed for manufacturing by rapid prototyping (Fig. 13 and 14). The elements corresponding to the force transmission, metrology and connection chains are glued together, with carbon rods to stiffen the sensor structure.

B. Sensor behavior with FEA

A moment M_y along the Y axis causes a displacement equal to $160\,\mu$m at the location of the sensing elements. The measurement amplitude of 500μm allows to perform the torque evaluation even in presence of additional moments of same amplitude in the X and Z directions, and forces equal to 100 N in the X and Z directions.

Considering the simultaneous application of moments equal to $5\,Nm$ along the X, Y and Z axes, and forces equal to 100N in the three directions, the maximal Von Mises equivalent stress is approximately equal to 30MPa, which remains compatible with the material used for rapid prototyping.

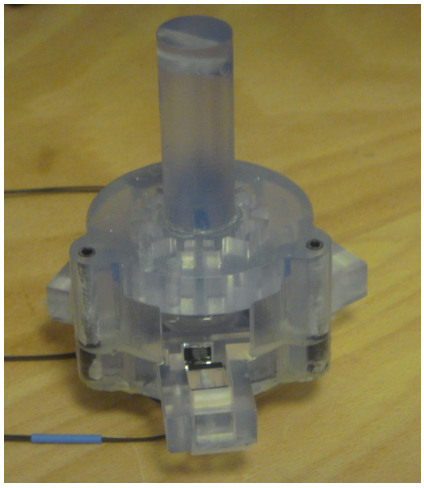

Fig. 15. Global view of the sensor obtained with rapid prototyping.

TABLE II
FEA and experimental displacement evaluation - 10N Load applied at 15 mm and 200 mm with respect to the sensor axis

Distance		Sensor 1	Sensor 2	Sensor 3
15 mm	FEA	-5μm	-16μm	12μm
	Exp.	-4μm	-16μm	9μm
200 mm	FEA	-47μm	-59μm	-33μm
	Exp.	-51μm	-48μm	21μm

The first two eigenfrequencies of the sensor are equal to 459 and 494 Hz. The eigenmodes correspond to the resonance of the legs of the metrology chain. The value of the first eigenfrequency seems compatible with the application.

C. Prototype and first experimental results

The prototype (Fig. 15) has been assembled, and a dedicated test bench needs yet to be designed for a fine evaluation. In particular, the relationship between the displacement measurements and the torque to be measured needs to be experimentally calibrated since for this prototype the sensor elements are not accurately positioned with respect to the structure.

First measurements however show that the displacements of the metrology end-effector are in accordance with numerical analysis. A 10N load has for instance been applied in a first step at 15 mm, and in a second step at 200 mm with respect to the sensor axis. The estimated displacements from FEA are indicated in table II as well as their experimental estimation.

V. Conclusion

In this paper, the design of a MRI-compatible torque sensor has been considered, using an optical measurement. The sensor has been designed focusing on the compliant structure needed for torque evaluation. Its architecture allows to tune separately the sensor stiffness, the sensor displacements for optical measurement, and cross-sensitivity has been optimized. Kinematic singularities are used to select

and design the compliant structures, and the behavior of the sensor has been analyzed using FEA. Further work will now include the quantitative evaluation of the first prototype. At the moment, the sensor may lack compactness because of the spatial arrangement of the kinematic chains. We therefore intend to redesign a second sensor, using the same kinematic principles, to get a more compact structure manufactured in a single element. That should in particular limit the existence of nonlinearities [27]. Then, the design of the sensor will be considered by optimizing simultaneously the selection of the optical sensor and the compliant structure.

REFERENCES

[1] A. Patriciu, D. Petrisor, M. Muntener, D. Mazilu, M. Schar, and D. Stoianovici, "Automatic brachytherapy seed placement under MRI guidance," *IEEE Transactions on Biomedical Engineering*, vol. 54, no. 8, pp. 1499–1506, 2007.

[2] I. Bricault, N. Zemiti, E. Jouniaux, C. Fouard, E. Taillant, F. Dorandeu, and P. Cinquin, "Light puncture robot for CT and MRI interventions," *IEEE Engineering in Medicine and Biology Magazine*, vol. 27, no. 3, pp. 42–50, 2008.

[3] C. Lebosse, P. Renaud, B. Bayle, and M. de Mathelin, "Nonlinear modeling of low cost force sensors," in *IEEE International Conference on Robotics and Automation*, 2008, pp. 3437–3442, Pasadena, USA.

[4] J. Z. Liu, T. H. Dai, T. H. Elster, V. Sahgal, R. W. Brown, and G. H. Yue, "Simultaneous measurement of human joint force, surface electromyograms, and functional MRI-measured brain activation," *Journal of Neuroscience Methods*, vol. 101, no. 1, pp. 49–57, Aug. 2000.

[5] U. Spaelter, D. Chapuis, R. Gassert, R. Moser, and H. Bleuler, "A versatile MRI/fMRI compatible spherical 2-dof haptic interface," in *IEEE/RAS-EMBS International Conference on Biomedical Robotics and Biomechatronics*, 2006, pp. 727–732, Pisa, Italy.

[6] H. H. Ehrsson, A. Fagergren, T. Jonsson, G. Westling, R. S. Johansson, and H. Forssberg, "Cortical activity in precision-versus power-grip tasks: An fMRI study," *J Neurophysiol*, vol. 83, no. 1, pp. 528–536, 2000.

[7] D.-H. Kim, "Real-time frequency compensatory filter for adjusting dynamic bandwidth of single-degree-of-freedom sensor system," *Sensors and Actuators A: Physical*, vol. 140, no. 2, pp. 251–256, 2007.

[8] M. Remouche, R. Mokdad, M. Lahrashe, A. Chakari, and P. Meyrueis, "Intrinsic optical fiber temperature sensor operating by modulation of the local numerical aperture," *Opt. Eng.*, vol. 46, no. 2, pp. 024 401–15, 2007.

[9] Y.-L. Park, K. Chau, R. Black, and M. Cutkosky, "Force sensing robot fingers using embedded fiber Bragg grating sensors and shape deposition manufacturing," in *IEEE International Conference on Robotics and Automation*, 2007, pp. 1510–1516, Roma, Italy.

[10] Y.-L. Park, S. C. Ryu, R. Black, B. Moslehi, and M. Cutkosky, "Fingertip force control with embedded fiber bragg grating sensors," in *IEEE International Conference on Robotics and Automation*, 2008, pp. 3431–3436, Pasadena, USA.

[11] M. Q. Feng and D.-H. Kim, "Novel fiber optic accelerometer system using geometric moiré fringe," *Sensors and Actuators A: Physical*, vol. 128, no. 1, pp. 37–42, 2006.

[12] S. Hirose and K. Yoneda, "Development of optical six-axial force sensor and its signal calibration considering nonlinear interference," in *IEEE International Conference on Robotics and Automation*, 1990, pp. 46–53 vol.1.

[13] K. Chinzei, N. Hata, F. A. Jolesz, and R. Kikinis, "MR compatible surgical assist robot: System integration and preliminary feasibility study," in *Proceedings of the Third International Conference on Medical Image Computing and Computer-Assisted Intervention*. Springer-Verlag, 2000, pp. 921–930.

[14] R. Gassert, R. Moser, E. Burdet, and H. Bleuler, "MRI/fMRI-compatible robotic system with force feedback for interaction with human motion," *IEEE/ASME Transactions on Mechatronics*, vol. 11, no. 2, pp. 216–224, 2006.

[15] F. Aghili and M. B. J. M. Hollerbach, "A joint torque sensor for robots," in *ASME International Mechanical Engineering Congress & Exposition*, 1997.

[16] N. Takahashi, M. Tada, J. Ueda, Y. Matsumoto, and T. Ogasawara, "An optical 6-axis force sensor for brain function analysis using fMRI," in *Proceedings of IEEE Sensors*, vol. 1, 2003, pp. 253–258 Vol.1.

[17] M. Tada, S. Sasaki, and T. Ogasawara, "Development of an optical 2-axis force sensor usable in MRI environments," in *Proceedings of IEEE Sensors, 2002*, vol. 2, 2002, pp. 984–989 vol.2.

[18] W. Lorenz, M. Peshkin, and J. Colgate, "New sensors for new applications: force sensors for human/robot interaction," in *IEEE International Conference on Robotics and Automation*, vol. 4, 1999, pp. 2855–2860 vol.4.

[19] D. Chapuis, R. Gassert, L. Sache, E. Burdet, and H. Bleuler, "Design of a simple MRI/fMRI compatible force/torque sensor," in *IEEE/RSJ International Conference on Intelligent Robots and Systems*, vol. 3, 2004, pp. 2593–2599 vol.3, Sendai, Japan.

[20] N. Lobontiu, *Compliant Mechanisms - design of flexure hinges*, C. Press, Ed., 2003.

[21] L. Lahousse, J. David, S. Leleu, G.-P. Vailleau, and S. Ducourtieux, "Application of a new architecture design to a measuring machine with a nanometric resolution," *Revue franaise de métrologie*, vol. 4, pp. 35–43, 2005.

[22] C. Gosselin and J. Angeles, "Singularity analysis of closed-loop kinematic chains," *IEEE Transactions on Robotics*, vol. 6, no. 3, pp. 281–290, 1990.

[23] R. Ranganath, P. S. Nair, T. S. Mruthyunjaya, and A. Ghosal, "A force-torque sensor based on a Stewart platform in a near-singular configuration," *Mechanism and Machine Theory*, vol. 39, no. 9, pp. 971–998, Sept. 2004.

[24] R. Stoughton and T. Arai, "Kinematic optimization of a chopsticks-type micromanipulator," in *Japan-USA Symp. on Flexible Autom.*, 1992, pp. 151–157.

[25] W. Bachta, P. Renaud, E. Laroche and J. Gangloff, "Cardiolock2: Parallel singularities for the design of an active heart stabilizer" in *IEEE International Conference on Robotics and Automation*, 2009, pp. 3839–3844, Kobe, Japan.

[26] S. Ronchi, O. Company, S. Krut, F. Pierrot, and A. Fournier, "High resolution flexible 3-RRR planar parallel micro-stage in near singular configuration for resolution improvement," in *IEEE International Conference on Industrial Technology*, 2005, pp. 395–400.

[27] D. Tsetserukou and S. Tachi, "Torque sensors for robot joint control", pp. 15–36, In J.G. Rocha and S. Lanceros-Mendes (Eds), *Sensors, Focus on Tactile, Force and Stress Sensors*, I-Tech Education and Publishing, 2008.